First-principles phase-stability study of fcc alloys in the Ti-Al system

Mark Asta and Didier de Fontaine
Department of Materials Science and Mineral Engineering, University of California, Berkeley, California 94720
and Materials Science Division, Lawrence Berkeley Laboratory, Berkeley, California 94720

Mark van Schilfgaarde
SRI International, Menlo Park, California 94025

Marcel Sluiter
Lawrence Livermore National Laboratory, Condensed Matter Division (L268), P.O. Box 808, Livermore, California 94550

Michael Methfessel
Fritz-Haber-Institute, Faradayweg 4-6, 1000, Berlin-33, Germany
(Received 3 December 1991; revised manuscript received 30 March 1992)

We present the results of a first-principles study of the composition-temperature phase diagram for fcc-based Ti-Al alloys and the related structural and thermodynamic properties. In the approach taken in this study, local-density-functional theory is combined with the formalism of the cluster-variation method (CVM). In particular, the formation energy, bulk modulus, and atomic volume of metastable fcc Ti, fcc Al, and nine ordered fcc intermetallic Ti-Al compounds have been calculated using the full-potential linear-muffin-tin-orbital method. It is shown how the results of these calculations can be used to obtain a set of volume-dependent effective cluster interactions (ECI's) which parametrize the total energies of fcc-based Ti-Al alloys. We discuss in detail how these parameters can be used to determine formation energies, atomic volume, and bulk moduli for both ordered and disordered alloys, and as an example we calculate these properties for alloys containing random distributions of Ti and Al atoms as a function of composition. Furthermore, these ECI's are used in conjunction with the CVM to calculate the solid-state, fcc, composition-temperature phase diagram.

I. INTRODUCTION

Ordered intermetallic compounds possess many properties which make them attractive as potential high-temperature structural materials. In particular, the strong bonding between unlike atoms in many of these compounds leads to high melting points and large elastic moduli, implying high strength at elevated temperatures. However, a major barrier to the widespread use of ordered intermetallics is that most of them lack room-temperature ductility and/or toughness.[1-3]

The ordered intermetallic compounds found in the Ti-Al system are particularly promising for aerospace applications because in addition to their excellent high-temperature properties, these alloys are about half as dense as the Ni-based superalloys which have traditionally been used in this industry. For this reason, much research has been directed at trying to improve the ductility of the Ti_3Al, TiAl, and $TiAl_3$ compounds without appreciably altering the other excellent mechanical properties. In particular, the effect of stoichiometry, ternary additions, and processing conditions upon the properties of these alloys is being investigated.[1-3]

Of primary importance in attempting to engineer the properties of the Ti-Al compounds is an understanding of the equilibrium and metastable phases in this system and their range of (meta)stability with respect to experimentally controlled parameters such as composition (c) and temperature (T). For this reason, the equilibrium c-T phase diagram for this system has been extensively studied and much research involving techniques such as rapid solidification has been directed at trying to examine metastable structures. Furthermore, the effect of the structure of the alloys on the mechanical and thermodynamic properties must also be understood in order to guide research on this system.

A thorough assessment of the experimental work which has been performed to study the equilibrium and metastable phases in this system can be found in Ref. 4, from which the phase diagram in Fig. 1 is redrawn. Solid and dashed lines in Fig. 1 indicate phase boundaries which are, respectively, either well determined or conjectured based upon incomplete experimental evidence. From Fig. 1 we see that for compositions less than approximately 10 at. % Al, α-Ti is in equilibrium, which has the hcp structure and which transforms to the bcc β phase at high temperatures. For compositions between 25 and 35 at. % Al, α_2 (Ti_3Al), which forms in the $D0_{19}$ superstructure of the hcp lattice, is found to be stable. α_2 undergoes a solid-state order-disorder transformation to α at roughly 1400 K. For larger concentrations of Al, the equilibrium phases all form in fcc-based structures, some of which are described in Fig. 2. In particular, the γ (TiAl) compound forms in the $L1_0$ structure and is stable over an extended composition range. At 75 at. % Al a $D0_{22}$ structure is stable in only a very small compo-

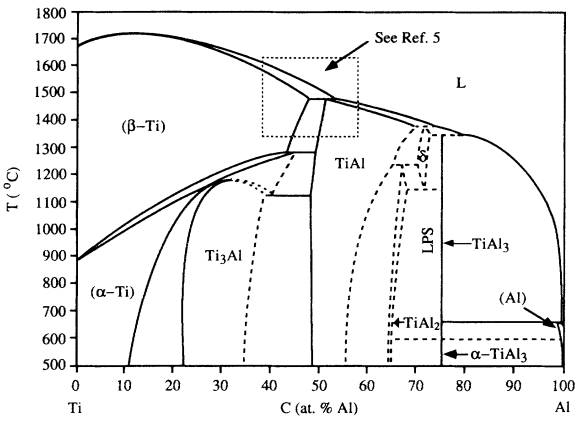

FIG. 1. Experimental Ti-Al phase diagram redrawn from Murray (Ref. 4). Solid and dashed lines indicate phase boundaries which are, respectively, well determined or conjectured based upon incomplete experimental evidence. The dashed square surrounds a part of the phase diagram which has been shown to be incorrect, and currently accepted phase boundaries are given in Ref. 5.

sition range. Both the TiAl and $TiAl_3$ compounds remain ordered up to their melting points. The dashed box in Fig. 1 surrounds a portion of the phase diagram which has now been shown to be incorrect. Currently accepted equilibrium phase boundaries can be found in Ref. 5.

The portion of the phase diagram between 55 and 75 at. % Al in Fig. 1 is not as well established experimentally as the rest. In particular, at composition $TiAl_2$ two phases have been observed with structures which are described by Loiseau *et al.*[6] as consisting of nonconservatively antiphased $L1_2$ unit cells. According to Murray[4] the details of the transformations between these phases are unresolved at present. Furthermore, an ordered Ti_3Al_5 superstructure was reported to have been observed by Miida, Hashimoto, and Watanabe.[7] However, a more recent study has concluded that this compound is not stable.[8] Also, the region labeled δ in Fig. 1 as well as the portion of the phase diagram labeled "LPS" contain long-period superlattice structures which can be described as consisting of one-dimensionally, conservatively antiphased $L1_2$ unit cells.[7–10] The reason for the relative stability of these phases and the particular sequences of these structures which are seen in this and other systems has been the subject of much theoretical and experimental work.[6,11–14] Finally, at low temperatures and at 75 at. % Al, van Loo and Rieck[10] have found evidence for the existence of a compound with a structure different from that of the $D0_{22}$, although more experimental work is needed to better characterize this phase and its possible stability.

Metastable phase equilibria have been investigated near the βTi→αTi transition as well as in the region of Al-rich alloys.[15,16] Additionally, evidence for a metastable Ti_3Al $L1_2$ phase has been found.[16] The existence of a metastable $L1_2$ phase is consistent with the *ab initio* calculations of Hong *et al.*,[17] which show that this fcc superstructure at composition Ti_3Al is only very slightly less energetically stable (less than 1 mRy/atom) than the equilibrium $D0_{19}$ structure.

Several *ab initio* electronic structure calculations[18,19] have been undertaken to better understand the stability of the various Ti-Al compounds. These studies have

Special Point Ordering Wave Vector	<0 0 0>	<1 0 0>		<1 1/2 0>			<1/2 1/2 1/2>
Name	FCC	$L1_2$	$L1_0$	$D0_{22}$	"40"	"$MoPt_2$-type"	$L1_1$
Formula	A	A_3B	AB	A_3B	AB	A_2B	AB
(1 0 0) Projections	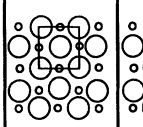	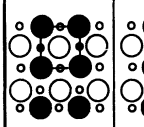	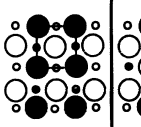	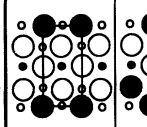	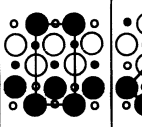	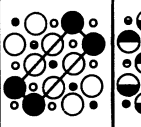	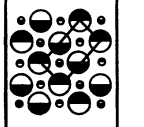
Prototype	Cu	Cu_3Au	CuAu	$TiAl_3$	—	$MoPt_2$	CuPt
Space Group	$Fm\bar{3}m$	$Pm\bar{3}m$	P4/mmm	I4/mmm	$I4_1/amd$	Immm	$R\bar{3}m$
Struckturbericht	A1	$L1_2$	$L1_0$	$D0_{22}$	—	—	$L1_1$
Pearson Symbol	cF4	cP4	tP4	tI8	tI8	oI6	hR32
Bravais Lattice	face centered cubic	simple cubic	simple tetragonal	body centered tetragonal	body centered tetragonal	body centered orthorhombic	rhombohedral
Unit Cell Vectors	[1 0 0] [0 1 0] [0 0 1]	[1 0 0] [0 1 0] [0 0 1]	[1 0 0] [0 1 0] [0 0 1]	[1 0 0] [0 1 0] [0 0 2]	[1 0 0] [0 1 0] [0 0 2]	[1 0 0] [0 -1/2 1/2] [0 3/2 3/2]	[1 0 0] [0 -1/2 1/2] [0 1 1]

FIG. 2. Description of the fcc-based structures considered in this study. (100) projections indicate atomic positions in the structures projected onto the (100) plane. Empty circles symbolize *A* atoms and filled circles are for *B* atoms. The smaller circles in these projections denote atoms which are displaced by $[\frac{1}{2}00]$ above the atoms denoted by larger circles. Half-filled circles denote atomic positions which are alternately occupied by *A* and *B* atoms along the [100] direction. Unit-cell vectors are given in terms of the conventional fcc unit cell.

shown that the bonding in this system is characterized by d(Ti-)-d(Ti) and d(Ti)-p(Al) electronic interactions, the latter becoming more important as the Al concentration is increased, and that the bonding is highly directional for Al-rich compositions.[17,20–22] In particular, the bonding between second-neighbor Ti atoms is important for the stability of the $D0_{19}$ structure at Ti_3Al,[17] while at $TiAl_3$ second-neighbor Ti-Al bonds lead to the stability of the $D0_{22}$ structure for which hybridization between p(Al) and d(Ti) electrons is enhanced.[20] The importance of the Ti-Al bonds for the stability of the $D0_{22}$ $TiAl_3$ phase is thought to be the reason for the strong effect which tetragonal distortion has on the total energy of this structure.[20,23,24] Furthermore, Chubb, Papaconstantopoulos, and Klein[26] have shown that the fact that the c/a ratio of $L1_0$ TiAl is greater than one can be explained by the nature of the Ti-Ti bonding in this structure.

Electronic-structure calculations have also been used to understand the structural and mechanical properties of the Ti-Al compounds. For example, among other properties, the equilibrium lattice parameters,[17,20–26] elastic moduli,[17,20–22,26] antiphase boundary (APB) energies,[21,22] heats of formation,[17,20–26] and the energy associated with the creation of twins in various Ti-Al structures[21,23] have been determined and calculated values are found to be in excellent agreement with experimental observations and measurements. A major limitation of these calculations is that only stoichiometric compounds at zero temperature are considered. The effect of variations in composition and temperature on the stability and structural and mechanical properties of a given compound cannot readily be taken into account. For this reason, Morinaga *et al.*[27] have performed calculations on Ti-Al clusters using the discrete variational (DV)-$X\alpha$ method[28] to examine the effect of the Al concentration and ternary additions on the electronic structure of the $L1_0$ TiAl phase; these authors conclude that the experimental observation that this phase is more brittle at Al-rich compositions can be understood by the fact that the addition of Al enhances the p-d bonding effects.

In this paper we present preliminary results of an *ab-initio* study of the c-T phase diagram in the Al-Ti system. In such a study, the relative stability of the hcp-, bcc-, and fcc-based structures in this system must be understood and as a first step we consider only the fcc-based compounds. The formation energies of the structures described in Fig. 2 have been calculated using the full-potential linear-muffin-tin-orbital (FP-LMTO) method[29] in order to study which of these are energetically favored. The fcc superstructures in Fig. 2 include those which are known to be stable, namely the $D0_{22}$ and $L1_0$, as well as several which are not experimentally observed. The energies of these nonequilibrium structures are needed in order to obtain a set of effective cluster interactions[30–32] (ECI's) which parametrize the total energy of this alloy system.

ECI's can be used in conjunction with the cluster-variation method[33] (CVM) to determine many thermodynamic and structural properties as a function of composition and temperature for both (partially) ordered and disordered alloy phases. In particular, in this paper we will show how these interaction parameters can be used to determine the volume, formation energy, bulk modulus, and free energy for any configuration of atoms in an alloy system. As an example, these properties will be calculated for alloys containing completely random distributions of Al and Ti atoms as a function of concentration, and the effect of atomic ordering and composition can then be examined. Furthermore, the solid-state, fcc phase diagram will also be computed.

The remainder of this paper is organized as follows: in Secs. II and III the details of the electronic structure calculations, the method of obtaining a set of ECI's, and the calculation of the phase diagram are discussed. The results of the FP-LMTO calculations are then given and are used to obtain a set of ECI's. Finally, results obtained with these interaction parameters, including the phase diagram, are presented and discussed.

II. ELECTRONIC STRUCTURE CALCULATIONS

Our purpose in performing total-energy calculations of Ti-Al fcc superstructures in this paper is to obtain a set of ECI's which can be used to study phase stability and the effect of composition and the state of order on the properties of the compounds in this alloy system. For this reason, the number of superstructures for which these total-energy calculations must be performed is equal to (or greater than) the number of ECI's which we expect to be important for describing the energetics of this system. In particular, the stability of a $D0_{22}$ relative to an $L1_2$ structure, such as is experimentally observed at 75 at. % Al in this system, can only be modeled by a set of ECI's which include interaction parameters beyond the range of the nearest-neighbor pair of the fcc lattice. Since there are ten distinct clusters of atoms within the range of the second-neighbor pair of the fcc lattice, the total energies of at least this many fcc superstructures must be calculated.

Furthermore, the effect of structural relaxation on the total energies of all of the fcc superstructures must be taken into account since these energies are to be used for the purpose of studying the relative stability of various alloy phases in this system. For example, previous studies have shown[21–24] that the $L1_2$ structure at 75 at. % Al is incorrectly predicted to be the more energetically stable phase in a first-principles total-energy calculation if the tetragonal distortion of the $D0_{22}$ structure is not taken into account.

In Sec. III it is shown that, provided total energies of "fully relaxed" ordered compounds are used to obtain the ECI's, the effect of structural relaxation will be included in the parametrization of the energy of a given alloy compound in terms of these interaction parameters. We must, therefore, find the minimum of the total energy with respect to all structural degrees of freedom for all of the ordered compounds, including those which are not experimentally observed.

A. Method

To calculate the total energies within the local density approximation[18,19] (LDA), we used the method of linear

muffin tin orbitals[34] (LMTO's), as it is known to be highly efficient and generally applicable. For the present work we used the full-potential version of the method,[29] as one of us has shown in detail[35] that employing the spherical approximation for the potential, as is customary in the LMTO and Korringa-Kohn-Rostoker (KKR) methods, does not produce sufficiently accurate results for the Ti-Al system. This is particularly true with respect to lattice distortions and associated energies of relaxation.

In these calculations, the local exchange-correlation potential of von Barth and Hedin[36] was used. The charge density was expanded to $l=6$ inside the spheres, though $l=4$ was found to be adequate to compare total-energy differences. In all cases, a basis set of 22 orbitals/atom was used, which entailed a tripling of the s and p orbitals and a doubling of the d orbitals. This was sufficient to converge the total energy with respect to basis to an absolute precision of approximately 1 mRy/atom; errors in energy differences are expected to be much smaller. With respect to the **k**-point summations, both sampling and tetrahedron schemes were used; the total energy was converged to approximately 0.03 mRy/atom in each case, with the number of irreducible **k** points being typically 300.

Both non-self-consistent and fully self-consistent calculations were carried out on each structure as a function of the atomic volume (Ω). For each volume, the structure was relaxed with respect to all degrees of freedom appropriate to it; for example the $D0_{22}$ was relaxed with respect to c/a. The equilibrium total energy (E_0), atomic volume (Ω_0), and bulk modulus (B) is then determined for each structure using a third-order fit of the total energy (E) to the atomic volume (Ω).

For the purpose of studying the relative stability of the different fcc superstructures, it is convenient to consider the formation energy [$\Delta E(\phi)$] of each structure (ϕ), which is defined as

$$\Delta E(\phi)=E_0(\phi)-c_\phi E_0(\mathrm{Al,fcc})-(1-c_\phi)E_0(\mathrm{Ti,fcc})\ , \tag{1}$$

where E_0(Al,fcc) and E_0(Ti,fcc) are the equilibrium total energies of fcc Al and fcc Ti, and where c_ϕ is the atomic concentration of Al in ϕ.

B. Description of structures

The fcc superstructures considered in this study are described in Fig. 2, and among them are those known to be stable or possibly metastable, i.e., the $L1_2$, $L1_0$, and $D0_{22}$, as mentioned in the Introduction. The ordered superstructures in Fig. 2 can be classified according to the dominant special-point ordering wave,[37,38] which is defined as the compositional **k** vector responsible for atomic ordering in the structure. On the fcc lattice there are three ordering wave families: $\langle 100\rangle$, $\langle 1\frac{1}{2}0\rangle$, and $\langle \frac{1}{2}\frac{1}{2}\frac{1}{2}\rangle$. The $L1_2$ and $L1_0$ structures belong to the $\langle 100\rangle$ family, the "$MoPt_2$ type," "40" ("40" is the number assigned to this structure by Kanamori and Kakehashi in Ref. 39), and $D0_{22}$ to $\langle 1\frac{1}{2}0\rangle$, and the $L1_1$ to the $\langle \frac{1}{2}\frac{1}{2}\frac{1}{2}\rangle$ family.[37]

From the experimental studies of phase stability in the Ti-Al system discussed in the Introduction, it can be concluded that $\langle 100\rangle$ and $\langle 1\frac{1}{2}0\rangle$ ordering waves are important in this system. Furthermore, most of the metastable and stable fcc superstructures observed in Ti-Al can be stabilized by nearest- and next-nearest-neighbor effective pair interactions.[37,39,40] We have included the 40, $MoPt_2$-type, and $L1_1$ structures in this study since they are also stabilized by first- and second-neighbor effective pair interactions[40] and because the first two belong to the relevant ordering wave families. These structures are candidate metastable phases in this system.

The space group symmetry of the structures given in Fig. 2 dictates the degrees of freedom for structural relaxation. The fcc and $L1_2$ have cubic symmetry and the only degree of freedom is the lattice parameter a. $D0_{22}$ and 40 are body-centered tetragonal while $L1_0$ is simple tetragonal; in these structures the [100] and [001] directions are not equivalent by symmetry and therefore the lattice parameters a and c need to be varied independently in the total-energy calculations. Although $L1_1$ is rhombohedral, we find that the unrelaxed structure (i.e., the one for which the atoms sit at the ideal fcc lattice sites) is the most energetically stable one so that only the effect on the total energy of the lattice parameter a is considered in this paper.

Finally, the $MoPt_2$-type structure is a body-centered orthorhombic one in which the three axes of the unit cell are not of the same length. For the ideal geometry (i.e., one which corresponds to the fcc lattice) we see that the lattice parameters a, b, and c, which describe the length along [100], $[0\ -\frac{1}{2}\ \frac{1}{2}]$ and [011], respectively, are related by $b/a=(1/2)^{1/2}$ and $c/a=(9/2)^{1/2}$. Furthermore, the distance between the A and B atoms at positions (0,0,0) and $(0,\frac{1}{2},\frac{1}{2})$ is not related to the lattice parameter c by symmetry; we calculate this distance at equilibrium to be $0.335c$ and $c/3$ for the $TiAl_2$ and Ti_2Al $MoPt_2$-type phases, respectively, where the latter value is the ideal one.

III. CLUSTER EXPANSIONS AND EFFECTIVE CLUSTER INTERACTIONS

The method described in Sec. II will be used to obtain the formation energies, bulk moduli, and equilibrium lattice parameters for stoichiometric compounds possessing translational symmetry. We now discuss how from these results a set of ECI's, which can be used to determine the same properties for an alloy with an arbitrary configuration of atoms, can be obtained.

A. Binary alloys and the Ising model

An exact description of the dependence of alloy properties on variables such as composition and temperature requires a knowledge of the partition function or, equivalently, the free energy of the system. Determining

these functions is an intractable problem for macroscopic systems and for this reason the Ising model is commonly used in theoretical studies of alloys.

As discussed in detail in Ref. 41, the only approximation which is made in formally mapping the real alloy onto an Ising lattice is that every microstate which is accessible to the system has an atomic configuration where each atom can unambiguously be assigned to a lattice point on a given lattice. Provided this can be done, to each state of the alloy system a configuration of spins (where an up spin symbolizes occupation by an A atom and a down spin corresponds to a B atom in an AB binary alloy system) on an appropriate Ising lattice can be assigned. In general, therefore, a given arrangement of Ising spins corresponds to many different states of the real alloy system. For example, in the present study a relaxed $MoPt_2$-type structure and one with an ideal fcc geometry would both be associated with same Ising spin configuration.

It can be shown[41] that at finite T the partition function of the alloy system can be reduced to that of the equivalent Ising model by integrating out the degrees of freedom associated with the many states corresponding to a given spin configuration. An approximate solution of the partition function of the Ising model, for example within the framework of the CVM, can then be used to determine the phase diagram as well as all related thermodynamic and structural properties.

B. Cluster expansions of the energy

As an example of the use of the Ising model, consider the formation energy (ΔE) for fcc-based Ti-Al alloys with a fixed atomic volume (Ω). From the model described in the Appendix, the formation energy is expressed as a function only of the average atomic volume and the configuration of the Ti and Al atoms on the *ideal fcc lattice*. The Ising model is defined by assigning spin values to the sites of the ideal fcc lattice which take on values $+1$ (-1) if an atom is occupied by an Al (Ti) atom. The set of spins defines the vector σ, which completely specifies the atomic configuration on the ideal fcc lattice. In short, using the model described in the Appendix, the formation energy is a function of Ω and σ only.

In order to determine the functional dependence of $\Delta E(\sigma,\Omega)$ on σ, the Ising lattice description is only useful if the coupling constants between the spin variables are specified and can be associated with the properties of the real system. A formally exact way of defining the interactions between pairs or, more generally, clusters of spins, is given in the paper of Sanchez, Ducastelle, and Gratias.[30] These authors show that any function of the Ising spin configuration σ can be expanded in terms of a complete orthonormal set of cluster functions. For a binary system on a lattice with N sites, there exists 2^N such cluster functions defined as

$$\Phi_\alpha=\sigma_{\mathbf{p}}\sigma_{\mathbf{p}'}\cdots\sigma_{\mathbf{p}''} , \tag{2}$$

where $\alpha=(\mathbf{p},\mathbf{p}',\ldots,\mathbf{p}'')$ defines a set of lattice points commonly referred to as a cluster and where $\sigma_{\mathbf{p}}$ is the spin variable which takes on values $+1$ or -1 depending on which type of atom is associated with site $\mathbf{p}$. In particular, the formation energy of the alloy at volume Ω can be expanded in terms of these cluster functions as follows:

$$\Delta E(\sigma,\Omega)=\sum_\alpha E_\alpha(\Omega)\Phi_\alpha(\sigma) , \tag{3}$$

where the $E_\alpha(\Omega)$ are the ECI's and are defined by

$$E_\alpha(\Omega)=\frac{1}{2^{n_\alpha}}\mathrm{Tr}_{\sigma_\alpha}\Phi_\alpha(\sigma_\alpha)\left[\frac{1}{2^{N-n_\alpha}}\mathrm{Tr}_{\sigma-\sigma_\alpha}\Delta E(\sigma,\Omega)\right] \tag{4}$$

with n_α and σ_α denoting the number of lattice points and the configuration of spins on the cluster α, respectively. The first trace in (4) is over the spin configurations of cluster α while the second trace is over all configurations of the lattice consistent with σ_α. Note that the ECI's are defined in terms of an average of the energy over all atomic configurations and are, therefore, *independent of* σ. A well known example of the expression (4) is that for the pair cluster:

$$E_{\mathbf{p},\mathbf{p}'}(\Omega)=\tfrac{1}{4}[E_{AA}(\Omega)+E_{BB}(\Omega)-2E_{AB}(\Omega)] , \tag{5}$$

where $E_{AA}(\Omega)$ is the average of $\Delta E(\sigma,\Omega)$ over all configurations containing A atoms at sites $\mathbf{p}$ and $\mathbf{p}'$ and similarly for $E_{BB}(\Omega)$ and $E_{AB}(\Omega)$.

At this point, expansion (3) does not simplify the problem of finding the value of $\Delta E(\sigma,\Omega)$ for an arbitrary configuration σ since the knowledge of 2^N ECI's is still required. However, as is shown in Refs. 41 and 30, the ECI's for clusters which are related by the space group symmetry of the *disordered lattice* (the fcc lattice in this study) are equivalent; this follows from the definition of the ECI's given in Eq. (4). Therefore, we can rewrite (3) by grouping equivalent terms together as

$$\Delta e(\sigma,\Omega)=\frac{1}{N}\Delta E(\sigma,\Omega)=\sum_\alpha{}' E_\alpha(\Omega)m_\alpha\overline{\Phi}_\alpha(\sigma) , \tag{6}$$

where the primed sum is over all clusters which are distinct by symmetry. m_α is the number of clusters α which are equivalent by symmetry divided by the number of sites N, and the overbar over the cluster function in (6) denotes that it is averaged over all of these equivalent clusters on the lattice. It is worth noting that in this study the ECI's in expansion (6) have the full symmetry of the fcc lattice even though the equilibrium structure of the real alloy corresponding to a given configuration σ may not.

The number of ECI's which must be determined in expansion (6) is still very large for a lattice describing a macroscopic system. Therefore, this expansion becomes useful if we assume that ECI's beyond a certain range and for clusters containing a large number of points are negligible. Recent studies[32,45] suggest that this assumption is a valid one. Therefore, we write

$$\Delta e(\sigma,\Omega)\approx\sum_\alpha^{\alpha_m}{}' E_\alpha(\Omega)m_\alpha\overline{\Phi}_\alpha(\sigma) , \tag{7}$$

where the sum is over a small set of clusters (α) up to some maximal one (α_m).

At this point, the problem of finding the equilibrium value of the total energy for a given configuration with an atomic volume Ω has been reduced to that of evaluating expansion (7). Two approximations which have been made in arriving at (7) should be noted. First of all, as discussed in the Appendix, we assume that the contribution to the formation energy of an alloy at fixed Ω associated with structural relaxation can be expressed as a function of σ and Ω only. Therefore, it is assumed that structural relaxation is in some sense small enough that in the relaxed state the position of the atoms can still be associated with the ideal fcc lattice sites and the atomic configuration can, therefore, be specified by σ. This assumption allows us to write the formation energy as a function of the configuration and the average atomic volume only. The configurational dependence of $\Delta e(\sigma,\Omega)$ can then be expressed in terms of an expansion in cluster functions associated with the ideal fcc lattice. The ECI's are the expansion coefficients which are defined in terms of an average over all atomic configurations of the formation energy, $\Delta e(\sigma,\Omega)$, according to Eq. (4). Therefore, the ECI's are independent of the atomic configuration and are functions only of the average atomic volume.

Another approximation made in using (7) to obtain the formation energy of an alloy system is that only a small set of ECI's are considered. This second approximation can be improved by including more ECI's in the expansion. Several other approximations are also commonly used in practice when calculating the ECI's. In the next section we describe a method for obtaining these interactions from the results of first-principles total-energy calculations for perfectly ordered stoichiometric alloy compounds.

C. Method for determining the effective cluster interactions

Provided that expansion (7) in terms of a subset of ECI's (Z in number) from the complete set gives an accurate description of the configurational dependence of the equilibrium energy, the formation energies of a set of ordered structures can be calculated and the resulting set of equations can be inverted to obtain the ECI's. This is the approach first implemented by Connolly and Williams.[42] As mentioned earlier, the effect of structural relaxation on the value of the ECI's must be included in order to correctly model phase stability of Ti-Al alloys; in Sec. III B, we showed that the model for alloy formation described in the Appendix allows us to include the effect of the energy of relaxation on these interaction parameters. In particular, the ECI's are determined at each volume in terms of formation energies of structurally relaxed alloys according to (4). Therefore, formation energies of completely relaxed ordered structures will be used to obtain the ECI's in this study.

In order to extract the ECI's, the set of ordered structures can be Z (the number of ECI's to be determined) in number, in which case the ECI's can be obtained by inverting (7) as follows:

$$E_\alpha(\Omega)=\frac{1}{m_\alpha}\sum_{\phi}^{Z}\Delta e(\phi,\Omega)\overline{\Phi}_\alpha^{-1}(\phi)\ , \tag{8}$$

where the interaction is defined in terms of a sum over the structures ϕ of the product of the equilibrium formation energies times a weight factor which is the inverse of the matrix of averaged cluster functions. Alternately, a set of X structural energies can be used with $X>Z$, in which case the ECI's can be obtained by minimizing the weighted variance:

$$\sum_{\phi}^{X}\omega_\phi\left[\Delta e(\phi,\Omega)-\sum_{\alpha}^{Z}m_\alpha E_\alpha(\Omega)\overline{\Phi}_\alpha(\phi)\right]^2=\text{Min}\ , \tag{9}$$

where the weights (ω_ϕ) are defined to be the number of variants of the structure ϕ on the lattice. For the fcc (and bcc) lattices we have

$$\omega_\phi=48N_C(\phi)/N_G(\phi) \tag{10}$$

with $N_C(\phi)$ and $N_G(\phi)$ being the number of atoms per unit cell and number of point group operations for ϕ, respectively. Formula (9) was suggested by Lu *et al.*[43] The values of ω_ϕ for the structures considered in this study are given in Table I.

A basic problem when ordered structural energies are

TABLE I. The average value of the 15 cluster functions considered in this paper and the weight variables $\omega(\phi)$ for the eleven structures described in Fig. 2. $\omega(\phi)$ is defined in Eq. (10).

									$\overline{\Phi}_\alpha$							
Structure	$\omega(\phi)$	1	2	3	4	5	6	7	8	9	10	11	12	13	14	15
fcc A	1	1	1	1	1	1	1	1	1	1	1	1	1	1	1	1
fcc B	1	1	−1	1	1	1	1	−1	−1	−1	−1	1	1	1	−1	1
$L1_2$ A_3B	4	1	$\frac{1}{2}$	0	1	0	1	$-\frac{1}{2}$	$\frac{1}{2}$	$-\frac{1}{2}$	$\frac{1}{2}$	−1	0	1	$\frac{1}{2}$	1
$L1_2$ AB_3	4	1	$-\frac{1}{2}$	0	1	0	1	$\frac{1}{2}$	$-\frac{1}{2}$	$\frac{1}{2}$	$-\frac{1}{2}$	−1	0	1	$-\frac{1}{2}$	1
$L1_0$ AB	6	1	0	$-\frac{1}{3}$	1	$-\frac{1}{3}$	1	0	0	0	0	1	$-\frac{1}{3}$	1	0	1
$D0_{22}$ A_3B	12	1	$\frac{1}{2}$	0	$\frac{2}{3}$	$\frac{1}{3}$	$\frac{1}{3}$	$-\frac{1}{2}$	$\frac{1}{6}$	$-\frac{1}{6}$	$-\frac{1}{6}$	−1	$-\frac{1}{3}$	$\frac{1}{3}$	−1	0
$D0_{22}$ AB_3	12	1	$-\frac{1}{2}$	0	$\frac{2}{3}$	$\frac{1}{3}$	$\frac{1}{3}$	$\frac{1}{2}$	$-\frac{1}{6}$	$\frac{1}{6}$	$\frac{1}{6}$	−1	$-\frac{1}{3}$	$\frac{1}{3}$	1	0
40 AB	12	1	0	$-\frac{1}{3}$	$\frac{1}{3}$	$\frac{1}{3}$	$-\frac{1}{3}$	0	0	0	0	1	$\frac{1}{3}$	$-\frac{1}{3}$	0	−1
$MoPt_2$ A_2B	18	1	$\frac{1}{3}$	$-\frac{1}{9}$	$\frac{1}{9}$	$\frac{1}{3}$	$-\frac{1}{9}$	$-\frac{1}{3}$	$\frac{1}{9}$	$\frac{1}{9}$	$-\frac{7}{9}$	$-\frac{1}{3}$	$-\frac{1}{9}$	$\frac{1}{9}$	$\frac{1}{3}$	1
$MoPt_2$ AB_2	18	1	$-\frac{1}{3}$	$-\frac{1}{9}$	$\frac{1}{9}$	$\frac{1}{3}$	$-\frac{1}{9}$	$\frac{1}{3}$	$\frac{1}{9}$	$-\frac{1}{9}$	$\frac{7}{9}$	$-\frac{1}{3}$	$-\frac{1}{9}$	$\frac{1}{9}$	$-\frac{1}{3}$	1
$L1_1$ AB	8	1	0	0	−1	0	1	0	0	0	0	−1	0	1	0	−1

used to calculate ECI's is that these interaction parameters are not uniquely determined. In other words, the values of the ECI's may differ according to the set of structures used. This is particularly the case if the number of ordered formation energies is equal to the number of ECI's determined through Eq. (8); by using a large set of ordered formation energies, checks can be made as to how well the ECI's describe $\Delta e(\phi,\Omega)$ for structures not used to calculate these interactions.

In this study, the ECI's and $\Delta e(\phi,\Omega)$ are taken to have a quadratic volume dependence, as suggested in (the appendix of) Ref. 44 (a quadratic fit is found to be sufficiently accurate over the volume range of interest in the study of this alloy system due to the small difference in the molar volumes of Ti and Al). The equilibrium energies of the structures described in Fig. 2 have been calculated as a function of atomic volume and the results are fit to the form:

$$\Delta e(\phi,\Omega)=A_0(\phi)+A_1(\phi)\Omega+A_2(\phi)\Omega^2 , \tag{11}$$

where

$$\begin{aligned} A_0(\phi)&=\Delta e_0(\phi,\Omega_0)+\tfrac{1}{2}B(\phi)\Omega_0(\phi) , \\ A_1(\phi)&=-B(\phi), \quad A_2(\phi)=\frac{B(\phi)}{2\Omega_0(\phi)} , \end{aligned} \tag{12}$$

and $B(\phi)$ and $\Omega_0(\phi)$ are the bulk modulus and equilibrium atomic volume of structure ϕ, respectively. We assume the following functional dependence on Ω for the ECI's:

$$E_\alpha(\Omega)=a_0(\alpha)+a_1(\alpha)\Omega+a_2(\alpha)\Omega^2 , \tag{13}$$

where the coefficients $a_i(\alpha)$ are determined by minimizing the weighted variance:

$$\sum_{\phi}^{X}\omega_\phi\left[A_i(\phi)-\sum_\alpha m_\alpha a_i(\alpha)\overline{\Phi}_\alpha(\phi)\right]^2=\text{Min} , \tag{14}$$

by analogy with (9).

As pointed out by Ferreira, Wei, and Zunger,[45] we do not want the properties calculated with the ECI's to be too sensitive to errors in the formation energies of the ordered structures which are used to obtain the interactions. These authors introduce a quantity which can be used to determine the effect of these errors on the formation energy of the random configuration of atoms at $c=0.5$. However, this quantity can only be determined when (8) is used to obtain the ECI's and cannot be used as a criterion for choosing the optimal set of ECI's in this study (since the number of energies is larger than the number of ECI's being determined). Instead, we determine the orthogonality of the averaged cluster functions by calculating O, which is defined as:

$$O=\frac{1}{2X(X-1)}\sum_{\phi}^{X}\sum_{\phi'}^{X\prime}\sum_{\alpha}^{Z}\hat{\overline{\Phi}}_\alpha(\phi)\hat{\overline{\Phi}}_\alpha(\phi') , \tag{15}$$

where the primed sum excludes the structure ϕ. The circumflex on the averaged cluster function denotes that it is normalized as follows:

$$\hat{\overline{\Phi}}_\alpha(\phi)=\frac{\overline{\Phi}_\alpha(\phi)}{\left[\sum_{\alpha}^{Z}[\overline{\Phi}_\alpha(\phi)]^2\right]^{1/2}} . \tag{16}$$

The value of O can range between zero for a completely orthogonal set of cluster functions and one for a set consisting of cluster functions of identical structures.

The formation energies for a large set of structures can be calculated in order to use Eqs. (8) or (9) to obtain a set of ECI's in practice. Then, the averaged cluster functions for many clusters can be determined for each structure. The set of ECI's which will be used in (7) are then chosen as the ones which best describe the configurational dependence of $\Delta e(\sigma,\Omega)$ for these structures. This is the approach taken in the study by Ferreira, Wei, and Zunger,[45] where out of clusters 1–9 and 11 and 12 shown in Fig. 3, the optimum set of ECI's is found to consist of clusters 1–7 and 11 for the semiconductor alloy systems considered by these authors.

In Fig. 3 we describe the 15 clusters considered in this study and list the values of the multiplicity (m_α) for each. The averaged cluster functions for each structure are given in Table I. As was mentioned in the Introduction, many of the fcc phases which are observed in this system can be stabilized by first- and second-neighbor pair interactions, and for this reason all clusters within this range have been included in this study. Furthermore, several studies[32,45,46] have shown that the third- and fourth-neighbor pair ECI's are generally of the same order of magnitude as the second-neighbor pair interaction. Additionally, it has been shown that linear many-body cluster interactions are often sizable.[32,47] Therefore, the linear triplet, the third- and fourth-neighbor pair, and the triangle consisting of one third- and two first-neighbor pairs are considered as well in this study.

We have determined all subsets of n ECI's from the set of 15 clusters described in Fig. 3, where n ranges from 5 to 9. For a given n, the optimum set of cluster interactions has been chosen as the one which minimizes the predictive error in the energy according to (9) for the 11 structures considered in this paper. We find that for some values of n more than one set of ECI's have the same minimum predictive error and in these cases we choose the set which additionally has the minimum value of O. This most orthogonal set should have ECI's which are less sensitive to errors in the calculated values of e_0, Ω_0, and B for the ordered structures used to obtain these parameters. Furthermore, this set of clusters spans the greatest volume of configuration space.

D. Phase diagram calculation

If thermal (vibrational) effects on the energy and entropy of the alloy system are not taken into account and the electronic entropy is neglected, Eq. (7) can be used in conjunction with the CVM expressions for the configurational entropy of an Ising lattice to form an approximate free-energy functional for the real alloy. This functional can be expressed in terms of a linearly independent set of correlation functions (ξ_α) which are defined to be the ensemble averages of the cluster func-

tions (Φ_α).[30,48] The free energy and equilibrium atomic volume at a given composition and temperature can be obtained by minimizing the free-energy functional with respect to Ω and the set of correlation functions ξ_α. From the free energy, the equilibrium phase boundaries at a given temperature can be obtained using common tangent constructions in the usual way. The locus of these phase boundaries constitutes the binary c-T phase diagram.

In the present study, the tetrahedron-octahedron[48] approximation of the CVM has been used for the configurational entropy of the fcc Ising lattice. The free-energy functional has the following form:

$$F(\Omega,T)=\sum_{\alpha}^{\alpha_m}{}' E_\alpha(\Omega) m_\alpha \xi_\alpha - k_B T \sum_{\alpha\varepsilon(T+O)}{}' m_\alpha \gamma_\alpha \sum_{\sigma_\alpha} x_\alpha(\sigma_\alpha)\ln x_\alpha(\sigma_\alpha) , \tag{17}$$

where the first term represents the internal energy (expressed as a formation energy) and comes from the ensemble average of the expression for the energy, Eq. (7). The second term on the right-hand side of (17) gives the CVM expression for the configurational entropy; the first sum is over all subclusters of the tetrahedron and octahedron ($T+O$) and the second sum is over the possible configurations on these subclusters. The γ_α in (17) are the Kikuchi-Barker coefficients[33,49] and the $x_\alpha(\sigma_\alpha)$ are referred to as cluster probabilities and are the ensemble averages of the fraction of clusters α on the lattice which have the configuration σ_α. These cluster probabilities are linearly related to the correlation functions.[48] The primed sums in (17) are again over all clusters which are distinct by symmetry.

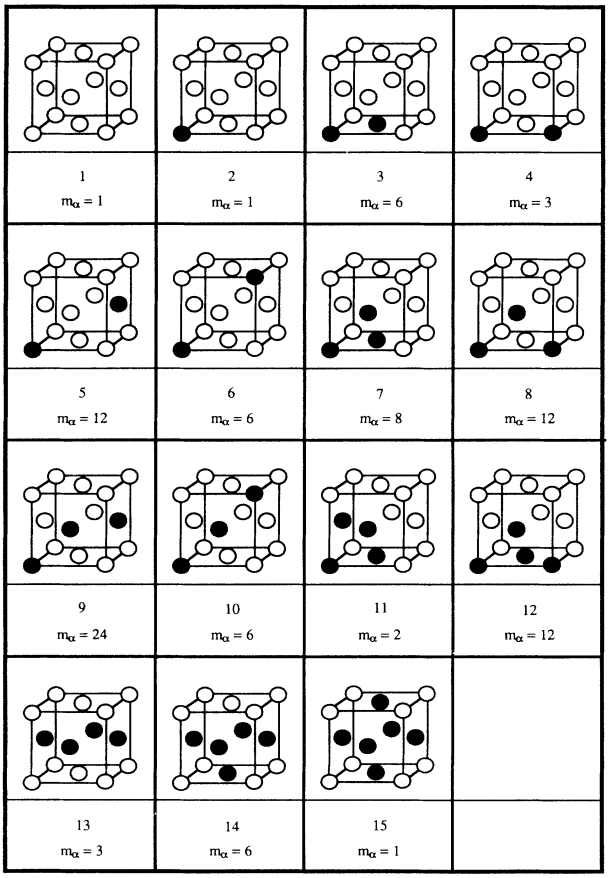

FIG. 3. Clusters considered in the expansion of the total energy. Filled circles denote the atoms in a given cluster. Cluster 1 is the "empty cluster" which corresponds to the constant (configurationally invariant) term in the expansion of the energy. m_α refers to the multiplicity of cluster α as defined in the text.

As we show in Sec. IV C, it is necessary to include ECI's for clusters which are not subclusters of the tetrahedron and octahedron (i.e., these ECI's correspond to clusters with a range larger than the second-neighbor pair of the fcc lattice) in order to parametrize well the energetics of the fcc superstructures in this system. For these clusters outside the range of the tetrahedron and octahedron, the value of the correlation function at a given concentration and temperature cannot be directly determined by minimizing Eq. (17). Therefore, for these clusters we express the correlation functions as linear combinations of products of the correlation functions of subclusters of the tetrahedron and octahedron by setting the cumulant of the cluster function equal to zero, as suggested by Carlsson[50] and Ferreira, Wei, and Zunger.[45]

E. Concentration dependence

From the minimization of the CVM free-energy functional (17), various thermodynamic and structural properties of an alloy phase can be determined as a function of composition and temperature. As an example, consider a completely random mixture of atoms on a lattice with an infinite number of sites (such a configuration of atoms will be referred to as a random alloy in the remainder of this paper). Such a state would be practically observed in a disordered alloy phase in the limit of very high temperatures where the entropy drives the thermodynamics. For such a random alloy the lattice averages of the cluster functions take on the following values:

$$\overline{\Phi}_\alpha(\text{rand.},c)=\langle\sigma\rangle^{n_\alpha}=(2c-1)^{n_\alpha} , \tag{18}$$

where we have used the fact that the average spin $\langle\sigma\rangle$ is related to the concentration c by $\langle\sigma\rangle=2c-1$. Therefore, for a random alloy, the expression for the energy takes the following form:

$$e_0(\text{rand.},\Omega)\approx\sum_{\alpha}^{\alpha_m}{}' E_\alpha(\Omega) m_\alpha (2c-1)^{n_\alpha} , \tag{19}$$

which is a polynomial in the concentration. The equilibrium atomic volume and bulk modulus for a random alloy at a given concentration can be determined from the first and second volume derivatives of Eq. (19), respectively. Examples of the concentration dependence of these properties for the Ti-Al system are given in Sec. IV F.

IV. RESULTS AND DISCUSSION

A. Results of electronic structure calculations

Table II lists the results of the present FP-LMTO electronic structure calculations of the formation energies, bulk moduli, and lattice constants of the fcc superstructures described in Fig. 2. It can be seen that the structures belonging to the $\langle 1\frac{1}{2}0 \rangle$ family are found to undergo structural relaxations further from the ideal fcc geometry than do those of the $\langle 100 \rangle$ and $\langle \frac{1}{2}\frac{1}{2}\frac{1}{2} \rangle$ families. For example, at 50 at. % Al the 40 structure has a c/a ratio which is 15% larger than ideal, while the equilibrium value for the $L1_0$ is only 1% larger than ideal and the $L1_1$ is found to undergo no structural relaxation.

The values of the formation energies are plotted versus the concentration of Al in Fig. 4, where it can be seen that among the structures considered here the most energetically stable intermetallic phases are the $L1_2$ Ti_3Al, $L1_0$ TiAl, and $D0_{22}$ $TiAl_3$ compounds. The 40, $D0_{22}$, and $L1_2$ structures are unstable at 50, 25, and 75 at. % Al, respectively, by only 2 mRy/atom (1 mRy/atom = 1.312... kJ/mole). The $L1_1$ structure is seen to be 17.6 mRy/atom less energetically stable than the $L1_0$. The $MoPt_2$-type Ti_2Al and $TiAl_2$ phases are unstable by 3.8 mRy/atom and 12.2 mRy/atom with respect to phase separation between the stable Ti_3Al and TiAl or $TiAl_3$ and TiAl compounds, respectively. In general, we see that at 25, 50, and 75 at. % Al the $\langle 1\frac{1}{2}0 \rangle$- and $\langle 100 \rangle$-type structures are all rather close in energy and that the latter are more stable at Ti-rich compositions. This reversal in the stability of the $\langle 100 \rangle$ family structures with respect to those of the $\langle 1\frac{1}{2}0 \rangle$ family can only be modeled by a set of ECI's which are either concentration-dependent and/or which include multiatom (i.e., more than two atoms) interactions.

The calculated molar volumes of the structures considered in this study are plotted in Fig. 5 as a function of the concentration of Al. From this plot we can see a significant deviation from Vegard's law by comparing the filled circles with the dashed line. The deviation is maximum at 75 at. % Al, where the $L1_2$ and $D0_{22}$ structures have volumes which are 6% and 5% smaller, respectively, than would be expected from Vegard's law. In general, the molar volume is a stronger function of composition than it is of the atomic structure at a given stoichiometry. This can be seen by noting that in going from 0 to 75 at. % Al we observed a 6% change in volume, while the maximum effect that the structure has on the volume at a given composition is the 3% difference between the $L1_1$ and $L1_0$ structures. Furthermore, it is seen that the highest symmetry structures have the smallest molar volumes at 25, 50, and 75 at. % Al and that these are also the most energetically stable with the exception of the $TiAl_3$ compounds.

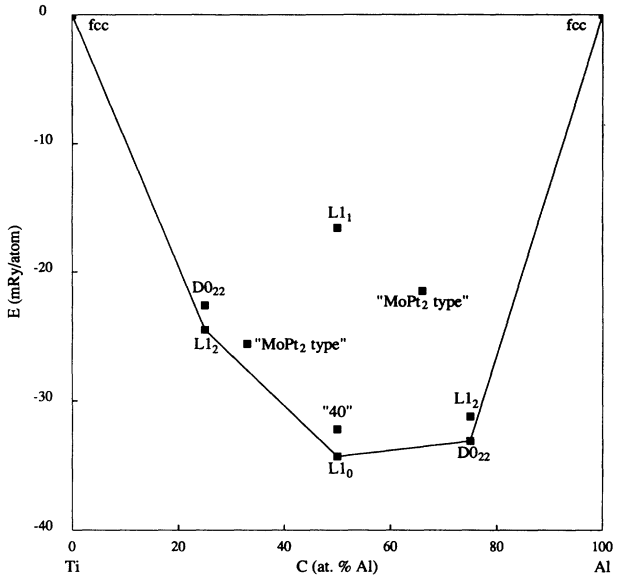

FIG. 4. Formation energies of fcc Ti-Al intermetallic compounds as calculated by the FP-LMTO method vs the atomic concentration of Al. The solid lines connect the energetically stable structures.

Figure 6 shows the dependence of the calculated bulk moduli on the concentration of Al. It can be seen that the addition of Al to pure Ti has a small effect on the bulk modulus while the opposite is true when Ti is added to Al. In fact, the bulk modulus of the $TiAl_3$ $D0_{22}$ compound is 50% larger than that of fcc Al, indicating that

TABLE II. Results of FP-LMTO calculations of equilibrium lattice constants, bulk moduli, and formation energies for fcc Al, fcc Ti, and nine fcc intermetallic Ti-Al compounds.

Composition	Structure	ΔE (mRy/atom)	B (Mbar)	R_{WS} (Å)	b/a	c/a
Ti	fcc		1.20	1.58		
Ti_3Al	$D0_{22}$	−22.6	1.27	1.56		2.12
Ti_3Al	$L1_2$	−24.6	1.27	1.55		
Ti_2Al	$MoPt_2$	−25.7	1.27	1.56	0.76	2.29
TiAl	$L1_1$	−16.6	1.17	1.56		
TiAl	40	−32.2	1.27	1.55		2.30
TiAl	$L1_0$	−34.2	1.28	1.54		1.01
$TiAl_2$	$MoPt_2$	−21.5	1.15	1.54	1.00	3.67
$TiAl_3$	$D0_{22}$	−33.0	1.18	1.54		2.24
$TiAl_3$	$L1_2$	−31.3	1.18	1.53		
Al	fcc		0.84	1.56		

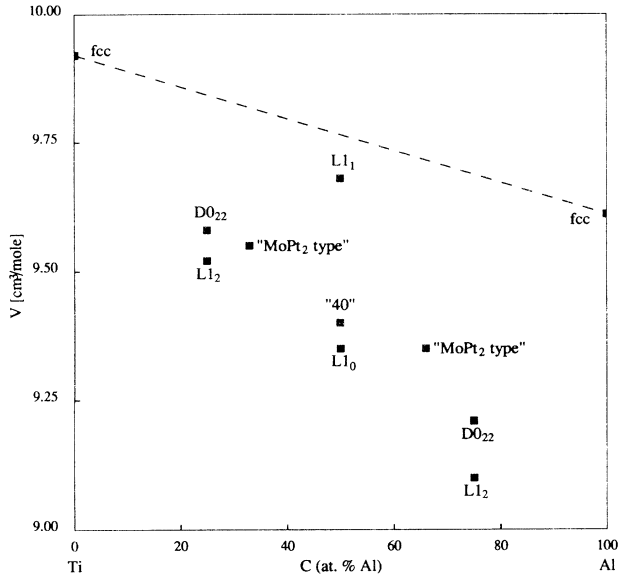

FIG. 5. Calculated molar volumes of fcc Ti-Al intermetallic compounds vs atomic concentration of Al for the 11 fcc structures considered in this study. The dashed line indicates the functional dependence of the molar volume on concentration expected from Vegard's law.

the *d* electrons of Ti have a strong effect on the bonding in this system, as was noted by Fu.[22]

B. Discussion of electronic structure calculations

As mentioned in the Introduction, many electronic structure calculations of Ti-Al intermetallic compounds have been undertaken for the purpose of understanding the relative stability and mechanical properties of these alloys. It is not our purpose to reproduce the results of these calculations in this paper, but, rather, to calculate

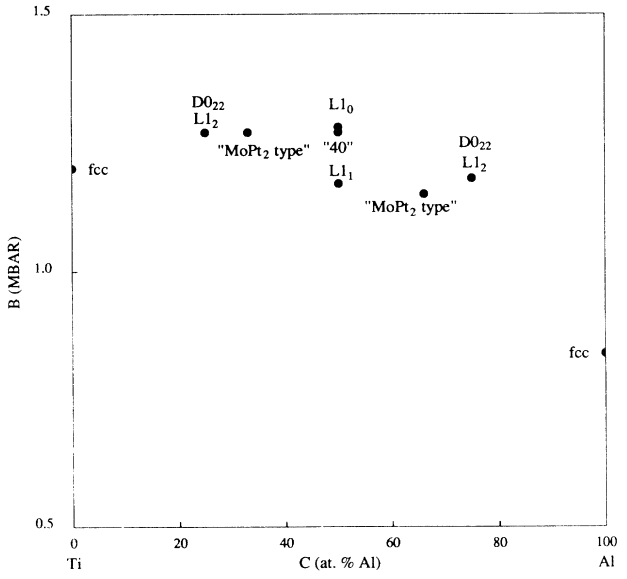

FIG. 6. Calculated bulk moduli of fcc Ti-Al intermetallic compounds vs the atomic concentration of Al for the 11 fcc structures considered in this study.

the total energies of a large number of fcc superstructures for the purpose of obtaining a set of ECI's which describe well the energetics of fcc Ti-Al alloys. Nevertheless, it is interesting to compare our results to those of previous calculations and to experiment as given in Table III in order to examine the agreement between the different computational approaches and experiment.

In general, we see that excellent agreement with previous calculations is obtained. In particular, values of the bulk moduli calculated here agree well with the full-potential linearized-augmented-plane-wave (FLAPW) calculations, as well as LMTO calculations in the atomic sphere approximation (ASA), and FP-LMTO results of Refs. 17, 20–22, 26, and 52 for all compounds given in Table II except for $L1_2$ $TiAl_3$. For this $L1_2$ structure, our calculated bulk modulus agrees completely with the FLAPW result of Ref. 22 *but* is 7% larger and 21% smaller than the FLAPW and LMTO-ASA results of Refs. 21 and 20, respectively. A comparison can be made between the calculated value of the bulk modulus and an experimentally measured value for pure fcc Al. In Ref. 51 (see references therein for experimental results), Sluiter *et al.* give a compilation of experimentally determined bulk moduli for Al extrapolated to $T=0$ K and show that the average of the measured values is 0.822 Mbar, which is within 10% of our calculated value of 0.84 Mbar.

The present results for the Wigner-Seitz radius (R_{WS}) agree to within 1% of those determined using the FLAPW,[17,21,22,26] and another version of the FP-LMTO approach.[52] Our calculated values of R_{WS} are 2% smaller than the experimental values,[53] as is commonly found in calculations that make use of the LDA. The LMTO-ASA calculations[17,20] give consistently larger values of R_{WS} which are in somewhat better agreement with experiment than our own and the other full-potential calculations just mentioned. We consider this fact to be fortuitous due to the shape approximations to the potential made in the case of the ASA. For the $D0_{22}$ structures, our calculated values of c/a given in Table II are within 2% of the results of Refs. 17, 22, and 23 and 1% of the experimental result[53] for $TiAl_3$. For the $L1_0$ our calculated c/a is in complete agreement with the previous FP-LMTO calculation,[52] is 3% smaller than the result of Chubb, Papaconstantopoulos, and Klein,[26] and is less than 1% smaller than the experimentally determined value.

The structural energy difference between the $D0_{22}$ and $L1_2$ structures can also be compared with previous calculations. At composition Ti_3Al the difference in energy between these structures was found to be $\Delta e_0(D0_{22},Ti_3Al)-\Delta e_0(L1_2,Ti_3Al)=1.5$ mRy/atom by Hong *et al.*,[17] in excellent agreement with the present results. At 75 at. % Al it is found that $\Delta e_0(D0_{22},TiAl_3)-\Delta e_0(L1_2,TiAl_3)=-3.7$ mRy/atom, -2.2 mRy/atom, -3.7 mRy/atom, and -4.0 mRy/atom in Refs. 20, 22, 25, and 23, respectively. Of these, the FLAPW results of Ref. 22 agree best with our own, while those of the ASA calculations[20,23,25] are about twice as large.

Hence, we find excellent agreement between the results

TABLE III. Results of previous first-principles electronic structure calculations and experimentally measured values of the bulk modulus and lattice parameters for fcc Ti-Al structures.

Composition	Structure	B (Mbar)	R_{WS} (Å)	c/a
Ti_3Al	$D0_{22}$	1.2[a,b]	1.56,[a] 1.58[b]	2.131[a]
Ti_3Al	$L1_2$	1.2[a,b]	1.56,[a] 1.58[b]	
TiAl	$L1_0$	1.26[c] 1.27[h] 1.24[d]	1.54[d,h]	1.01[d] 1.037[h]
			(1.57[i])	(1.016[i])
$TiAl_3$	$D0_{22}$	1.2,[e] 1.18[c,g]	1.54,[c,g] 1.55[e] (1.56[i])	2.21,[f] 2.25[g] (2.234[i])
$TiAl_3$	$L1_2$	1.5,[e] 1.10,[c] 1.18[g]	1.53,[c,g] 1.54[e]	

[a]FLAPW results of Ref. 17.
[b]LMTO-ASA results of Ref. 17.
[c]FLAPW results of Ref. 21.
[d]FP-LMTO results of Ref. 52.
[e]LMTO-ASA results of Ref. 20.
[f]LMTO-ASA with Ewald correction results from Ref. 23.
[g]FLAPW results of Ref. 22.
[h]FLAPW results of Ref. 26.
[i]Experimentally measured results of the lattice parameter according to Ref. 53.

of our own calculations and those obtained with the FLAPW method and another FP-LMTO method in particular. The agreement between our results and the experimental values of R_{WS} and B is also quite good in the cases where comparisons have been made. Furthermore, the fact that we find the $L1_2$ Ti_3Al, $L1_0$ TiAl, and $D0_{22}$ $TiAl_3$ compounds to be the most stable among those fcc superstructures considered in this study agrees with the experimental evidence for the metastability[16] of the first and stability[4] of the second and third phases.

C. Effective cluster interactions

We have determined the optimum sets of ECI's containing between five and nine of the interactions corresponding to the clusters described in Fig. 3 using the method discussed in Sec. III C. From these sets of ECI's the formation energies, equilibrium volumes, and bulk moduli of the 11 structures were determined by making use of (7) and the first and second volume derivatives of this expansion. The weighted root-mean-square (rms) error involved in predicting these properties was then calculated according to (9). Table IV shows the results of these calculations for the optimal sets of ECI's which gave the smallest predictive error in the formation energies. In addition, the value of O (which is related to the orthogonality of the cluster functions) and the formation energy of the random alloy at $c=0.5$ are also given in this table.

From Table IV we see that the value of the predictive error in the energies decreases monotonically as the number of clusters in the expansion is increased as does the value of O. Furthermore, the prediction of the atomic volume also improves as the number of ECI's is increased, except in going from six to seven interactions, and the predictive error in the bulk modulus is around 3% for six or more interactions. Finally, note that the

TABLE IV. Results of ECI determination for sets of clusters containing between five and nine interactions. The set of ECI's listed in this table are the optimum ones according to the criteria discussed in the text. Predictive errors for the formation energies, molar volumes, and bulk moduli are given as well as the formation energy of the random alloy at 50 at. % Al. The value of the orthogonality parameter O defined in the text is also given for these sets of ECI's.

	rms predictive errors				
Clusters	Δe_0 (mRy/atom)	V (cm^3/mole)	B (Mbar)	Δe(rand.,$c=0.5$) (mRy/atom)	O
1 2 3 4 11	2.6	0.102	0.06	−20.7	0.547 44
1 2 3 4 7 11	2.3	0.021	0.03	−20.7	0.499 78
1 2 3 4 10 11 14	1.7	0.075	0.04	−20.7	0.411 92
1 2 3 4 7 10 11 14	1.1	0.012	0.03	−20.7	0.381 79
1 2 3 4 7 10 11 14 15	0.3	0.009	0.03	−21.0	0.305 32

formation energy of the random alloy at $c=0.5$ is predicted to be the same by all sets of ECI's except for the final set of nine, for which it changes by less than 1 mRy/atom, indicating that the expansion for this random alloy is well converged.

The set of nine interactions listed at the bottom of Table IV has been used in the remainder of this paper since for this set of ECI's the predictive error in the energy is less than 1 mRy/atom (which is one-half of the smallest structural energy difference for the fcc superstructures considered). In Fig. 7 we show that the values of the formation energies predicted by this set of ECI's are very close to those determined from the FP-LMTO calculations, and the relative stability of the fcc structures is well reproduced.

We find that the optimum set of nine interactions in this system consists of the empty cluster, the nearest- and next-nearest-neighbor pairs, the nearest-neighbor isosceles triangle, the linear triplet, the nearest-neighbor regular tetrahedron, the pyramid, and the octahedron. It is interesting to note that this set of ECI's is different than the set which was found in Ref. 45 for semiconductor alloys and which has been used successfully to determine the ground states of many intermetallic systems.[43,54] First of all, we find that nine instead of eight interactions are needed to characterize accurately the formation energies of the structures considered in this system. Furthermore, the third- and fourth-neighbor pair interactions are not found to be important in describing the total energy of the alloys in this system. From these observations it seems that the choice of the optimal set of ECI's is, in general, dependent on the system under study. Also, we find that the linear triplet ECI is important, in agreement with the results of Wolverton *et al.*[32] and Bieber and Gautier.[47] This interaction was not considered by Ferreira, Wei, and Zunger.[45]

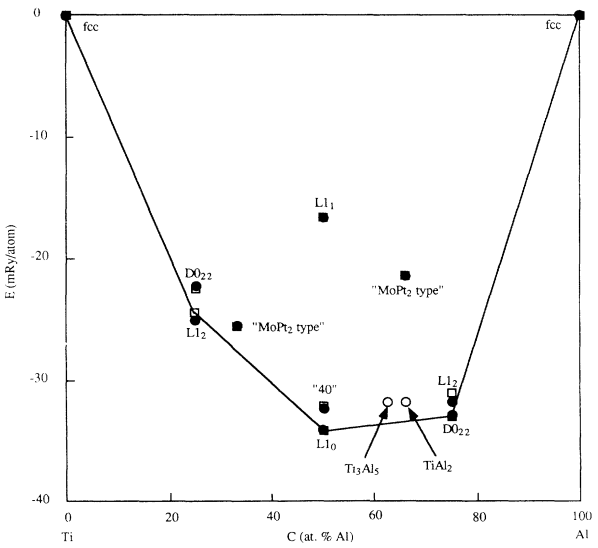

FIG. 7. Predicted formation energies from the nine ECI's listed in Table 5. Open squares indicate the FP-LMTO results and filled circles indicate predicted values from the cluster expansion of the energy (7). Open circles indicate predicted formation energies, from the cluster expansion, for the experimentally observed Ti_3Al_5 and $TiAl_2$ phases.

In Table V the values of the coefficients $a_i(\alpha)$ defined in Eq. (13) are given for the optimum set of nine ECI's. In addition, the values of these ECI's at $\Omega=9.68$ cm^3/mole (the calculated equilibrium molar volume of the $L1_0$ structure) are also given. We find that, except for the empty and point clusters, the two largest ECI's are those for the nearest- and next-nearest-neighbor pairs. Also, the pyramid and octahedron interactions are quite large in magnitude, indicating the importance of many-body ECI's in this system.

The range of interest of the molar volume for the Ti-Al system is between 9 and 10 cm^3/mole. In Table V we also indicate the absolute value of the difference between the maximum and minimum value of each ECI ($|\Delta E_\alpha|$) in this range of volumes. We can see from the values of $|\Delta E_\alpha|$ that the dominant contributions to the volume dependence of the energy of the alloy come from the empty and point ECI's. All ECI's except the one corresponding to the configurationally independent term in the energy $[E_0(\Omega)]$ are observed to change monotonically in this volume range.

D. Ground states on the fcc lattice

The results of Sec. IV A have shown that of the structures considered in the band-structure calculations, the $L1_2$ structure at 25 at. % Al, the $L1_0$ at 50 at. % Al, and the $D0_{22}$ at 75 at. % Al are the most stable fcc superstructures. The ECI's can be used to perform a complete ground-state search to find those structures which are energetically stable at $T=0$ K out of all possible atomic configurations. Such a study has been undertaken by Lu and co-workers[43,54] and Wolverton *et al.*[55] for other metallic alloy systems. In this paper, a complete ground-state search is complicated by the volume dependence of the ECI's and has not yet been undertaken. Instead, we will use the ECI's to check whether the experimentally observed phases between 55 and 75 at. % Al are predicted to be stable in this system. It should be emphasized that once a suitable set of ECI's has been determined, the formation energies of any fcc superstructure, regardless of the size of the unit cell, can be determined so that no further electronic structure calculations are required. Furthermore, the effect of structural relaxation on these formation energies is included since these ECI's were determined using energies of "fully relaxed" ordered structures.

At composition $TiAl_2$ two phases (the phase boundaries of these compounds are shown as dashed lines in Fig. 1) have been observed, which can be described as being made up of nonconservatively antiphased $L1_2$ unit cells, with each one displaying a different periodicity of these APB's.[6] According to Loiseau *et al.*,[6] at low temperatures the $ZrGa_2$ prototype structure is the stable one while at higher temperatures the $HfGa_2$ prototype is found. These two compounds are degenerate in energy when described by ECI's up to the range of the eighth-neighbor pair so that we find the same formation energy of -31.9 mRy/atom, bulk modulus of 1.2 Mbar, and molar volume of 9.23 cm^3/mole for each.

TABLE V. Volume dependence and values of ECI's for the optimum set of nine interactions given in Table IV. Coefficients $a_i(\alpha)$ give the functional dependence of the ECI's on the molar volume, as discussed in the text. $|\Delta E_\alpha|$ is the absolute value of the difference between the minimum and maximum values of the interaction for cluster α in the molar volume range 9–10 cm^3/mole. Additionally, $E_\alpha(V=9.68$ cm^3/mole) is the value of each ECI at the calculated molar volume of the $L1_0$ TiAl phase.

Cluster	$a_1(\alpha)$ (mRy)	$a_2(\alpha)$ (mRy mole/cm^3)	$a_3(\alpha)$ (mRy mole^2/cm^6)	$E_\alpha(V=9.68$ cm^3/mole) (mRy)	$\lvert\Delta E_\alpha\rvert$ (mRy)
1	378.95	−83.69	4.39	−20.19	1.30
2	−43.93	5.53	−0.16	−5.64	2.44
3	−4.24	2.25	−0.14	4.06	0.49
4	2.92	−1.60	0.11	−2.32	0.47
7	−1.20	0.46	−0.03	0.32	0.14
10	0.05	−0.18	0.01	−0.59	0.05
11	0.71	0.22	−0.02	0.65	0.22
14	−4.08	1.11	−0.06	1.09	0.02
15	−2.77	0.81	−0.04	1.64	0.11

The calculated formation energy of these $TiAl_2$ compounds are plotted in Fig. 7 (indicated as $TiAl_2$), where it can be seen that although these $TiAl_2$ compounds are more stable than the $MoPt_2$ type, they are not found to be in equilibrium at $T=0$ K in this system, according to the present calculation. These $TiAl_2$ phases are unstable by only 1.8 mRy/atom with respect to phase separation between the $D0_{22}$ $TiAl_3$ and $L1_0$ TiAl compounds. Since it is likely that long-ranged effective cluster interactions not considered in this study are responsible for the stability of these $TiAl_2$ compounds, the value of 1.8 mRy/atom gives an idea of the contribution these ECI's make to the formation energy of the alloys in this system. This contribution is small compared to the formation energies of the fcc Ti-Al alloys and should therefore not affect the results of the phase diagram calculation to be discussed in Sec. IV E.

The cluster expansion can also be used to check the stability of the Ti_3Al_5 phase, which was claimed to be stable by Miida, Hashimoto, and Watanabe[7] and was later shown to be unstable.[8] We find that the formation energy of this structure is also −31.9 mRy/atom, and the bulk modulus and molar volume are 1.2 Mbar and 9.27 cm^3/mole, respectively. The calculated formation energy of this compound is also plotted in Fig. 7 (indicated as Ti_3Al_5) where it is shown that this phase is calculated to be unstable with respect to phase separation between the $L1_0$ TiAl and $ZrGa_2$-type $TiAl_2$ compounds at zero temperature by only 0.6 mRy/atom.

E. Phase diagram

The method described in Sec. III D has been used to calculate the solid-state, fcc, c-T phase diagram of the Ti-Al system. The set of nine interactions given in Table V has been used in this calculation and of these interaction parameters, only the one corresponding to cluster 10 (the linear triplet cluster) gives a term in the internal energy which is not included in the tetrahedron-octahedron approximation of the CVM. Therefore, the correlation function for the linear triplet cluster was treated in the manner discussed at the end of Sec. III D. In Sec. IV D we showed that among the fcc superstructures experimentally observed in this system, only the $L1_2$ Ti_3Al, $L1_0$ TiAl, and $D0_{22}$ $TiAl_3$ compounds are predicted to be stable at $T=0$ K by our total energy calculations, and only these ordered compounds and the fcc disordered phase are considered in our computation of the phase diagram.

The calculated phase diagram is shown in Fig. 8, which indicates that the $L1_2$ Ti_3Al and $L1_0$ TiAl phases are stable over an extended composition range up to the order-disorder transition temperatures of ~3100 K and

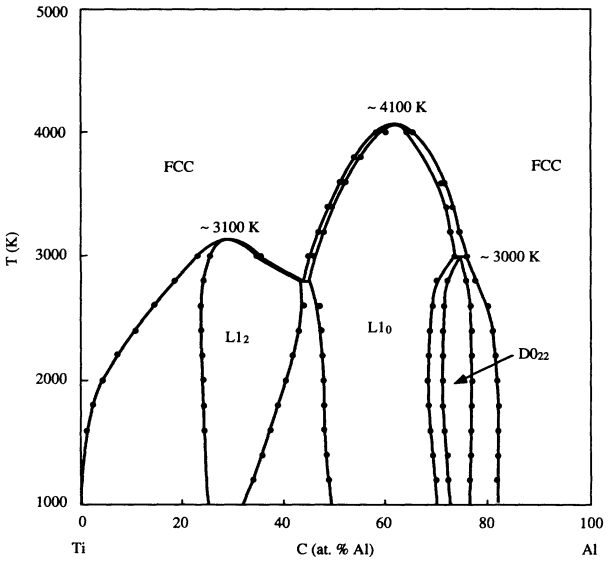

FIG. 8. Calculated composition-temperature phase diagram for fcc-based Ti-Al phases. The small dots correspond to calculated phase boundaries and the solid lines represent fits to these points. The stability regions for the ordered Ti_3Al, TiAl, and $TiAl_3$ compounds are indicated by the Strukturbericht designation for their structures: $L1_2$, $L1_0$, and $D0_{22}$, respectively. Temperatures in this figure refer to transitions from ordered phases to disordered fcc for the $L1_2$ and $L1_0$ structures and for the peritectoid reaction ($D0_{22}\rightarrow L1_0$+fcc) for the $D0_{22}$ structure.

~4100 K, respectively. The $D0_{22}$ $TiAl_3$ compound, by contrast, is found to be stable over a relatively small concentration range up to ~3000 K, where it undergoes a peritectoid reaction to $L1_0$+fcc.

The experimentally determined phase diagram shown in Fig. 1 contains phase boundaries between hcp, bcc, and liquid as well as fcc phases while only fcc phases are considered in our calculations. Therefore, a comparison between our computed phase diagram and experiment can be made only for Al-rich compositions. We predict that both the $L1_0$ TiAl and $D0_{22}$ $TiAl_3$ compounds are ordered well above their experimentally observed melting points, in agreement with the experimental phase diagram. Additionally, we find a much narrower concentration range for the stability of the $D0_{22}$ $TiAl_3$ than for the $L1_0$ TiAl compound, also in agreement with experimental observations. Furthermore, the small energy difference between the $D0_{22}$ and $L1_2$ $TiAl_3$ structures found in this study is indicative of a small (100) APB energy, which is consistent with the many experimentally observed one-dimensional long-period superstructures[7-10] in this system.

A shortcoming of the calculated phase diagram is our prediction that solid solution of Ti in Al is stable over an extended composition range at low temperatures while experimentally it is found that Ti is soluble only up to a maximum of 2 at. % below the melting point of Al. The stability of the disordered solid solution with respect to phase separation between the $D0_{22}$ $TiAl_3$ compound and pure fcc Al is also reflected in Fig. 9(a). In this figure it can be seen that the formation energy of the random alloy (indicated by the dashed line) is actually less than that of the phase-separated state (indicated by the solid line) between 90 and 100 at. % Al. The random alloy should not be stable at $T=0$ K, and indeed we have found that additional ordered phases are stabilized by our set of ECI's between 75 and 100 at. % Al. A ground-state search, such as has been undertaken in Refs. 43, 54, and 55, is needed to find which ordered structures are the lowest-energy ones in this composition range; the results of such an analysis is presently being undertaken.

The Ti-rich portion of the phase diagram contains hcp and bcc phases in reality so that the fcc solid solution and $L1_2$ Ti_3Al compound are actually unstable in this system. A comparison with the experimental phase diagram for concentrations less than 50 at. % Al will be possible when the hcp and bcc phases are included in our calculations.

F. Structural and thermodynamic properties of disordered alloys

The values of the formation energies, molar volumes, and bulk moduli for random Ti-Al alloys have been calculated from the optimum set of nine ECI's using Eq. (19) and the first and second volume derivatives of this expansion. In Figs. 9(a)–9(c) the values of these properties as a function of concentration are shown as dashed lines.

In Fig. 9(a) we see that the formation energy of the random alloy has a roughly parabolic dependence on the concentration, with a minimum near 60 at. % Al. From Eq. (19) we see that the formation energy of the random alloy is expressed as a polynomial in the concentration with an nth-order term, which has contributions from clusters with n or more points. Therefore, the roughly parabolic dependence of the formation energy of the random alloy on concentration is indicative that effective pair interactions dominate in this system. The filled squares in Fig. 9(a) indicate the FP-LMTO values of the formation energy for the $L1_2$ Ti_3Al, $L1_0$ TiAl, and $D0_{22}$ $TiAl_3$ compounds, which are the phases found to be most stable among those considered. The difference between the formation energy of an ordered structure and the random alloy at the same concentration is defined as the ordering energy:

$$\Delta e_{\rm ord}(\phi)=\Delta e_0(\phi)-\Delta e_0({\rm rand.},c_\phi)\ , \tag{20}$$

where the formation energies on the right-hand side of the equation are evaluated at the equilibrium volume of the ordered structure ϕ and of the random alloy, respectively. We find that the values of $\Delta e_{\rm ord}$ are 9.4 mRy/atom, 13.1 mRy/atom, and 13.5 mRy/atom for the $L1_2$ Ti_3Al, $L1_0$ TiAl, and $D0_{22}$ $TiAl_3$ compounds, respectively.

The open symbols in Fig. 9(a) are the heats of formation measured from calorimetry experiments.[56,57] In order to compare these experimental results with our calculated formation energies, we have used the energy difference between fcc and hcp Ti calculated with the FP-LMTO method in Ref. 35. This energy difference is needed for a comparison because the heats of formation are measured experimentally for alloys forming from hcp Ti and fcc Al. We find excellent agreement between the experimental heats of formation and the formation energies obtained from our calculations. For example, the experimental measurements show that the heat of formation is largest in magnitude at roughly 60 at. % Al, as we find to be true for the formation energy of the random alloy.

In Fig. 9(b) we see that even for the random alloy a significant deviation from Vegard's law is found for the molar volume versus concentration of Al. The molar volume of the random alloys are roughly 0.2 cm^3/mole larger than those of the stable ordered structures, as can be seen by comparing the dashed line with the filled squares in this figure. The open symbols again correspond to experimental measurements.[53] The fact that the experimentally determined molar volumes are larger than our calculated values is consistent with the fact that these measurements are made at elevated temperatures and the fact that the LDA calculations are known to underestimate the value of the lattice parameter by a few percent. The agreement with the experimental values can be made better by including an approximate correction for the vibrational entropy in our calculations, as has been done by Moruzzi, Janak, and Schwarz[58] and by Sanchez, Stark, and Moruzzi.[59] The experimentally observed concentration dependence of the molar volume is well described by our calculations, as can be seen by comparing the open and filled symbols. In particular, the molar volume is experimentally found to reach a minimum at 75 at. % Al, as we find to be true for the ordered and disordered al-

loys.

In Fig. 9(c) we again notice that the bulk modulus changes more upon the addition of Ti to Al than when Al is added to Ti even in the case of the random alloy, although the effect is not as strong as for the ordered compounds. Furthermore, we see that the random alloy consistently has a lower bulk modulus than that of the ordered intermetallic compounds in this system. By comparing Figs. 6 and 9(c) with Fig. 4, a correspondence can be established between the relative stability (energetically) of a set of phases and the magnitude of the bulk modulus at a given concentration. At 50 at. % Al the $L1_1$ is less stable energetically than the random alloy, which in turn is less stable than the 40 structure; the $L1_0$ is the most stable TiAl compound. These phases can be ordered in the same way according to the value of their bulk moduli.

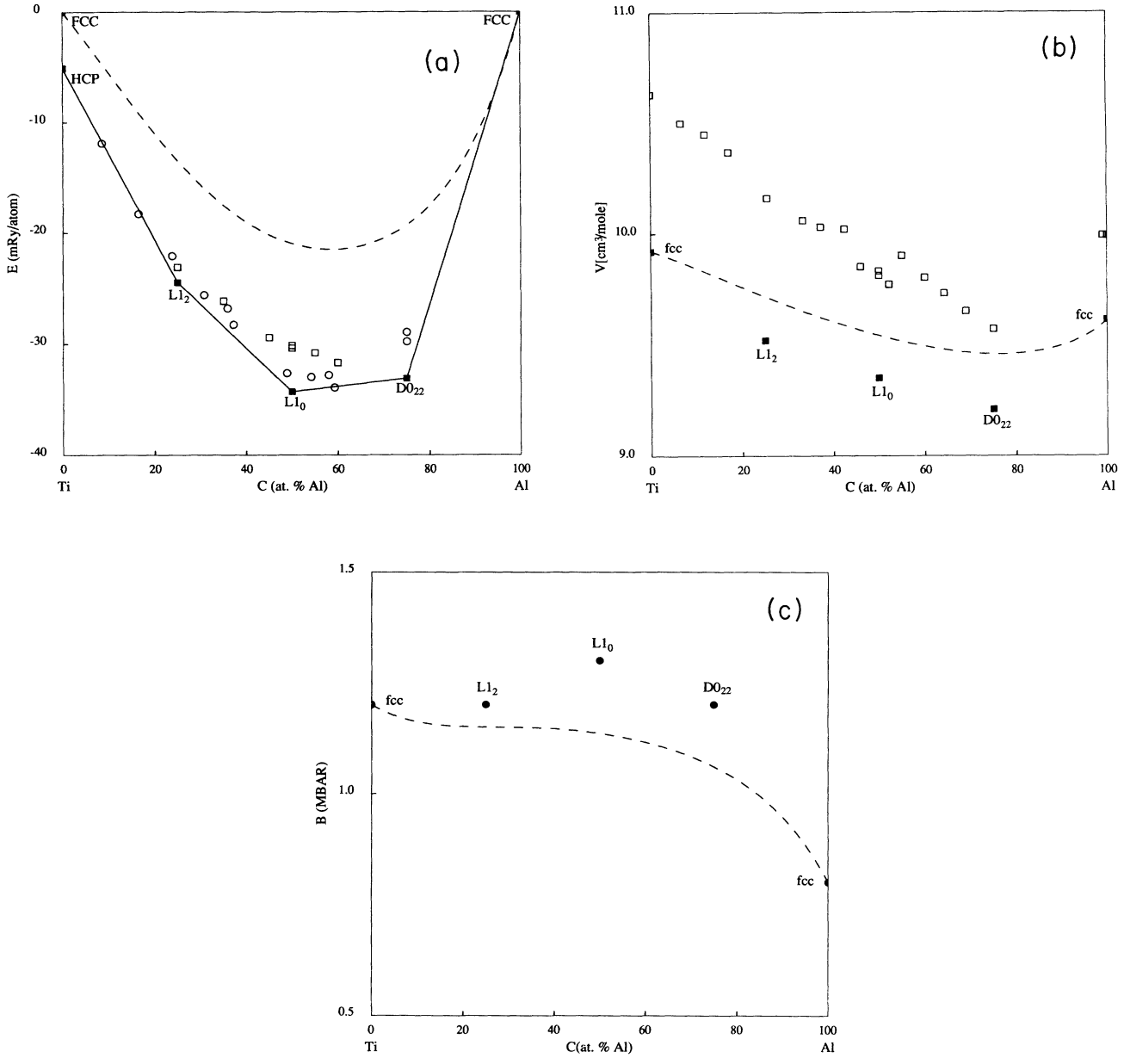

FIG. 9. Properties of random fcc Ti-Al alloys vs atomic concentration of Al obtained from the volume-dependent set of nine ECI's given in Table V. (a) Formation energies for the random alloys are indicated by the dashed line. Filled squares represent FP-LMTO results for the energetically stable structures. The energy difference between fcc and hcp Ti is taken from Ref. 35. Open squares and circles indicate experimentally measured heats of formation from Refs. 56 and 57, respectively. (b) Molar volumes of the random alloys are indicated by the dashed line. Filled squares represent FP-LMTO results for the energetically stable structures. Open squares denote the experimentally measured molar volumes from Ref. 53. (c) Bulk moduli for random alloys are indicated by the dashed line and solid circles symbolize the FP-LMTO results for the energetically stable structures.

A similar correspondence between the formation energy and the bulk modulus can be made at 25 and 75 at. % Al, so we can conclude that the more stable a structure is energetically at a given composition, the larger the bulk modulus will be.

V. SUMMARY

We have presented the results of a first-principles study of the phase stability and structural and thermodynamic properties of fcc-based phases in the Ti-Al system. The FP-LMTO approach has been used to calculate the formation energy, bulk modulus, and molar volume for fcc Ti, fcc Al, and nine fcc intermetallic Ti-Al compounds. Of the fcc superstructures studied the $L1_2$ Ti_3Al, $L1_0$ TiAl, and $D0_{22}$ $TiAl_3$ compounds are found to be most stable energetically. Therefore, as we go from pure fcc Ti to pure fcc Al, we find a reversal in the relative stability of $\langle 100 \rangle$ and $\langle 1\frac{1}{2}0 \rangle$ family structures due to the large structural relaxations these latter structures undergo at Al-rich concentrations. We find significant deviations from Vegard's law for the atomic volume, and the value of the bulk modulus is close to that of pure fcc Ti for all of the intermetallic compounds including Al-rich ones. Hence, it is clear that the composition has a nontrivial effect on the properties of this alloy system.

The results of these FP-LMTO calculations can be used in conjunction with an Ising-model description of the Ti-Al, fcc-based alloy system to determine structural and thermodynamic properties for any configuration of atoms. In particular, we have discussed in detail how total-energy calculations as a function of the atomic volume for perfectly ordered, stoichiometric compounds can be used to obtain volume-dependent ECI's, which can in turn be used to determine the formation energy, molar volume, and bulk modulus of any Ti-Al compound.

Because of the sizable dependence of many of the alloy properties on composition and atomic ordering, a large set of ECI's and, hence, a large number of total-energy calculations, are needed to parametrize the energetics of this system. Furthermore, the energy associated with structural relaxation in many of the noncubic Ti-Al fcc superstructures is very large and plays an important role in, for example, the stability of the $D0_{22}$ relative to the $L1_2$ structure at 75 at. % Al.[21–24] Therefore, this relaxation effect must be taken into account in our determination of the ECI's, and, hence, in our total-energy calculations. In other words, a large number of fully relaxed total-energy calculations are absolutely necessary in this study, and so is, therefore, a full-potential band-structure approach. The large computational effort is worthwhile considering that the result is a set of ECI's which can be used to determine the effect of composition and ordering on the formation energy, volume, and bulk modulus of any fcc-based alloy compound. In particular, these properties can be determined for phases which are only partially ordered or completely disordered.

The Ising-model description of this alloy system, together with the CVM, has been used to formulate a free-energy functional from which a composition-temperature phase diagram for the fcc-based Ti-Al phases has been calculated. The calculated phase diagram shows that the ordered fcc superstructures in this system are stable with respect to disordered solid solutions to very high temperatures (>3000 K), which is consistent with the fact that these compounds are experimentally observed to remain ordered up to their melting points. Furthermore, we find a much narrower composition range for the stability of the $D0_{22}$ $TiAl_3$ compound than for the $L1_0$ TiAl compound as is observed experimentally. In general, the agreement with experiment is encouraging, particularly since no adjustable parameters were used in our calculations.

As an example of how the Ising-model description allows the calculation of many properties of this alloy system, we have determined the effect of the concentration of Al on the properties of random alloys. The results obtained for the molar volume and formation energy show good agreement with the experimentally observed dependence of these properties on the composition. We are therefore encouraged to continue this study by including hcp and bcc phases as well as the fcc phases considered in this paper.

ACKNOWLEDGMENTS

One of the authors (M.A.) gratefully acknowledges helpful discussions with Dr. Prabhakar Singh, Chris Wolverton, Chris Walton, Ryan McCormack, and Professor Gerbrand Ceder. The research at the University of California was supported by the Director, Office of Energy Research, Office of Basic Energy Sciences, Materials Sciences Division of the U.S. Department of Energy under Contract No. DE-AC03-76F00098 and by the Institute for Scientific Computing Research at the Lawrence Livermore National Laboratory, Livermore, CA.

APPENDIX

Our model for the formation of an fcc-based Ti-Al alloy with a given configuration of Ti and Al atoms and a fixed average atomic volume is the following (which is closely related to the model described in Ref. 51): (1) An amount $(1-c)$ of fcc Ti is compressed or expanded to have the specified atomic volume (Ω). The same is done for an amount c of fcc Al. The total energy required is called the elastic energy, $E^{\text{elas}}(\sigma,\Omega)$. (Note that σ specifies the arrangement of the Ti and Al atoms on the ideal fcc lattice and also, therefore, the value of the concentration c.) (2) The Ti and Al atoms are mixed while remaining on the sites of an ideal fcc lattice with atomic volume Ω; the associated energy is the so-called chemical energy, $E^{\text{chem}}(\sigma,\Omega)$. (3) Finally, the atoms relax away from the ideal lattice sites in a manner which preserves the average atomic volume (Ω). In this model we will assume that the relaxations are in some sense small enough that the atoms can be uniquely assigned to the sites of the ideal fcc lattice and that the configuration of atoms is un-

changed due to relaxation. With this assumption, which will not be valid if a structural instability exists for some atomic configuration, the energy associated with relaxation, denoted as $E^{\text{relax}}(\sigma,\Omega)$, is a function of the configuration of atoms on the ideal fcc lattice and the average atomic volume only.

In summary, in this model for alloy formation the total formation energy can be written as a function of the average atomic volume and configuration only. The equilibrium value of the average atomic volume (Ω_0) will be the one which minimizes the total formation energy:

$$\Delta E(\sigma,\Omega)=E^{\text{elas}}(\sigma,\Omega)+E^{\text{chem}}(\sigma,\Omega)+E^{\text{relax}}(\sigma,\Omega)\ . \tag{A1}$$

The bulk modulus is defined in terms of the second derivative of Eq. (A1) with respect to Ω.

[1]Robert W. Cahn, Mater. Res. Bull. **16**, 18 (1991).

[2]R. L. Fleischer, D. M. Dimiduk, and H. A. Lipsitt, Annu. Rev. Mater. Sci. **19**, 231 (1989).

[3]M. Yamaguchi and Y. Umakoshi, Prog. Mater. Sci. **34**, 1 (1990).

[4]J. L. Murray, in *Phase Diagram of Binary Titanium Alloys,* edited by J. L Murray (ASM International, Metals Park, OH, 1987), pp. 12–24.

[5]C. McCullough, J. J. Valencia, C. G. Levi, and R. Mehrabian, Acta Metall. **37**, 1321 (1989).

[6]A. Loiseau, G. Van Tendeloo, R. Portier, and F. Ducastelle, J. Phys. (Paris) **46**, 595 (1985).

[7]R. Miida, S. Hashimoto, and D. Watanabe, Jpn. J. Appl. Phys. **21**, L59 (1982).

[8]A. Loiseau and A. Lasalmonie, Acta Crystallogr. Sec. B **41**, 411 (1985).

[9]A. Raman and K. Schubert, Z. Metallk. **56**, 44 (1965).

[10]F. J. J. van Loo and G. D. Rieck, Acta Metall. **21**, 73 (1973).

[11]G. Ceder, M. De Graef, L. Delaey, J. Kulik, and D. de Fontaine, Phys. Rev. B **39**, 381 (1989); G. Ceder, D. de Fontaine, H. Dreyessé, D. M. Nicholson, G. M. Stocks, and B. L. Gyorffy, Acta Metall. **38**, 2299 (1990).

[12]D. de Fontaine and J. Kulik, Acta Metall. **33**, 145 (1985); J. Kulik, Ph.D. thesis, University of California at Berkeley, Berkeley, 1988 (unpublished).

[13]H. Sato and R. Toth, in *Alloying Behavior and Effects in Concentrated Solid Solutions,* edited by T. B. Massalski (Gordon and Breach, New York, 1965), pp. 295–419; Phys. Rev. **127**, 469 (1962).

[14]J. Yeomans, Solid State Phys. **41**, 151 (1988).

[15]H. Bohner, Z. Metallk. **26**, 268 (1934); G. Falkenhagen and W. Hofmann, *ibid.* **43**, 69 (1952).

[16]T. Ohashi and R. Ichikawa, Z. Metallk. **64**, 517 (1973); J. Cisse, H. W. Kerr, and G. F. Bolling, Metall. Trans. **5**, 633 (1974); H. W. Kerr, J. Cisse, and G. F. Bolling, Acta Metall. **22**, 677 (1974).

[17]T. Hong, T. J. Watson-Yang, X.-Q. Guo, A. J. Freeman, T. Oguchi, and Jian-hua Xu, Phys. Rev. B **43**, 1940 (1991).

[18]P. Hohenberg and W. Kohn, Phys. Rev. B **136**, 864 (1964).

[19]W. Kohn and L. J. Sham, Phys. Rev. A **140**, 1133 (1965).

[20]T. Hong, T. J. Watson-Yang, A. J. Freeman, T. Oguchi, and Jian-hua Xu, Phys. Rev. B **41**, 12 462 (1990).

[21]M. H. Yoo and C. L. Fu (unpublished); C. L. Fu and M. H. Yoo, Philos. Mag. Lett. **62**, 159 (1990).

[22]C. L. Fu, J. Mater. Res. **5**, 971 (1990).

[23]D. M. Nicholson, G. M. Stocks, W. M. Temmerman, P. Sterne, and D. G. Pettifor, in *High Temperature Ordered Intermetallic Alloys III,* edited by C. T. Liu, A. I. Taub, N. S. Stoloff, and C. C. Koch, MRS Symposia Proceedings No. 133 (Materials Research Society, Pittsburgh, 1989), p. 17.

[24]Prabhakar P. Singh, M. Asta, D. de Fontaine, and M. van Schilfgaarde, in *Alloy Phase Stability and Design,* edited by G. M. Stocks, D. P. Pope, and A. F. Giamei, MRS Symposia Proceedings No. 186 (Materials Research Society, Pittsburgh, 1991), p. 41.

[25]A. E. Carlsson and P. J. Meschter, J. Mater. Res. **4**, 1060 (1989).

[26]S. R. Chubb, D. A. Papaconstantopoulos, and B. M. Klein, Phys. Rev. B **38**, 12 120 (1988); M. J. Mehl, J. E. Osburn, D. A. Papaconstantopoulous, and B. M. Klein, in *Alloy Phase Stability and Design* (Ref. 24), p. 277.

[27]M. Morinaga, J. Saito, N. Yukawa, and J. Adachi, Acta Mettall. **38**, 25 (1990).

[28]M. Morinaga, N. Yukawa, and H. Adachi, J. Phys. F **15**, 1071 (1985); M. Morinaga, N. Yukawa, H. Adachi, and T. Mura, *ibid.* **17**, 2147 (1987).

[29]M. Methfessel, Phys. Rev. B **38**, 1537 (1988).

[30]J. M. Sanchez, F. Ducastelle, and D. Gratias, Physica **128A**, 334 (1984).

[31]M. Asta, C. Wolverton, D. de Fontaine, and H Dreyssé, Phys. Rev. B **44**, 4907 (1991).

[32]C. Wolverton, M. Asta, H. Dreyssé, and D. de Fontaine, Phys. Rev. B **44**, 4914 (1991).

[33]R. Kikuchi, Phys. Rev. **81**, 988 (1951).

[34]O. K. Andersen, O. Jepsen, and D. Glötzel, in *Highlights of Condensed Matter Theory,* edited by F. Bassani *et al.* (North-Holland, Amsterdam, 1985).

[35]M. van Schilfgaarde, A. T. Paxton, A. Pasturel, and M. Methfessel, in *Alloy Phase Stability and Design* (Ref. 24), p. 107.

[36]U. von Barth and L. Hedin, J. Phys. C **5**, 1629 (1972).

[37]D. de Fontaine, Solid State Phys. **34**, 73 (1979).

[38]A. G. Khachaturayan, Phys. Status Solidi B **60**, 9 (1973).

[39]J. Kanamori and Y. Kakehashi, J. Phys. (Paris) Colloq. **38**, C7-274 (1977).

[40]M. Kaburagi and J. Kanamori, Prog. Theor. Phys. **54**, 30 (1979); M. J. Richard and J. W. Cahn, Acta Metall. **19**, 1263 (1971); S. M. Allen and J. W. Cahn, *ibid.* **20**, 423 (1972).

[41]G. Ceder, Ph.D. thesis, University of California at Berkeley, Berkeley, 1991 (unpublished).

[42]J. W. D. Connolly and A. R. Williams, Phys. Rev. B **27**, 5169 (1983); J. W. D. Connolly and A. R. Williams, in *The Electronic Structure of Complex Systems,* Vol. 113 of *NATO Advanced Study Institute, Series B: Physics,* edited by P. Phariseau and W. M. Temmerman (Plenum, New York, 1985), p. 581.

[43]Z. W. Lu, S.-H. Wei, Alex Zunger, S. Frota-Pessoa, and L. G. Ferreira, Phys. Rev. B **44**, 512 (1991).

[44]M. Sluiter and P. E. A. Turchi, Phys. Rev. B **40**, 11 215 (1989).

[45]L. G. Ferreira, Su-Huai Wei, and Alex Zunger, Phys. Rev. B **40**, 3197 (1989).

[46]F. Ducastelle, in *Phase Transformation in Solids,* edited by T. Tsakalakos (North-Holland, Amsterdam, 1984), p. 375; A.

Bieber, F. Gautier, G. Treglia, and F. Ducastelle, Solid State Commun. **39**, 149 (1981).
[47]A. Bieber and F. Gautier, J. Phys. Soc. Jpn. **53**, 2061 (1984).
[48]J. M. Sanchez and D. de Fontaine, Phys. Rev. B **17**, 2926 (1978).
[49]J. A. Barker, Proc. R. Soc. London, Ser. A **216**, 45 (1953).
[50]A. E. Carlsson, Phys. Rev. B **35**, 4858 (1987).
[51]M. Sluiter, D. de Fontaine, X. Q. Guo, R. Podloucky, and A. J. Freeman, Phys. Rev. B **42**, 10 460 (1990).
[52]P. K. Khowash, D. L. Price, and B. R. Cooper, in *Alloy Phase Stability and Design* (Ref. 24), p. 47.
[53]P. Villars and L. D. Calvert, *Pearson's Handbook of Crystallographic Data for Intermetallic Phases* (American Society for Metals, Metals Park, OH, 1985).
[54]Z. W. Lu, S.-H. Wei, A. Zunger, and L. G. Ferreira, Solid State Commun. **78**, 583 (1991).
[55]C. Wolverton, G. Ceder, D. de Fontaine, and H. Dreyssé, Phys. Rev. B **45**, 13 105 (1992).
[56]O. Kubaschewski and W. A. Dench, Acta Metall. **3**, 339 (1955).
[57]O. Kubashchewski and G. Heymer, Trans. Faraday Soc. **56**, 473 (1960).
[58]V. L. Moruzzi, J. F. Janak, and K. Schwarz, Phys. Rev. B **37**, 790 (1988).
[59]J. M. Sanchez, J. P. Stark, and V. L. Moruzzi, Phys. Rev. B **44**, 5411 (1991).